Optogenetic investigation of cardiac arrhythmia mechanisms

Feola, I.

Chapter 3

LOCALIZED OPTOGENETIC TARGETING OF ROTORS IN ATRIAL CARDIOMYOCYTE MONOLAYERS

Iolanda Feola[1], MSc; Linda Volkers[1], PhD; Rupamanjari Majumder[1], PhD; Alexander Teplenin[1], MSc; Martin J. Schalij[1], MD, PhD; Alexander V. Panfilov[1,2], PhD; Antoine A.F. de Vries[1], PhD; Daniël A. Pijnappels[1], PhD.

[1] Laboratory of Experimental Cardiology, Department of Cardiology, Heart Lung Center Leiden; Leiden University Medical Center, the Netherlands.
[2] Department of Physics and Astronomy, Ghent University, Ghent, Belgium.

Circ Arrhythm Electrophysiol 2017; 10:e005591

ABSTRACT

Background

Recently, a new ablation strategy for atrial fibrillation (AF) has emerged, which involves the identification of rotors (*i.e.* local drivers) followed by the localized targeting of their core region by ablation. However, this concept has been subject to debate since the mode of arrhythmia termination remains poorly understood, as dedicated models and research tools are lacking. We took a unique optogenetic approach to induce and locally target a rotor in atrial monolayers.

Methods and Results

Neonatal rat atrial cardiomyocyte monolayers expressing a depolarizing light-gated ion channel (Ca^{2+}-translocating channelrhodopsin [CatCh]) were subjected to patterned illumination to induce a single, stable and centralized rotor by optical S1-S2 cross-field stimulation. Next, the core region of these rotors was specifically and precisely targeted by light to induce local conduction blocks of circular or linear shapes. Conduction blocks crossing the core region, but not reaching any unexcitable boundary, did not lead to termination. Instead, electrical waves started to propagate along the circumference of block, thereby maintaining reentrant activity, although at lower frequency. If, however, core-spanning lines of block reached at least one unexcitable boundary, reentrant activity was consistently terminated by wave collision. Lines of block away from the core region resulted merely in rotor destabilization (*i.e.* drifting).

Conclusions

Localized optogenetic targeting of rotors in atrial monolayers could lead to both stabilization and destabilization of reentrant activity. For termination, however, a line of block is required reaching from the core region to at least one unexcitable boundary. These findings may improve our understanding of the mechanisms involved in rotor-guided ablation.

Keywords

Ablation, atrial fibrillation, cardiomyocytes, optogenetics, optical mapping.

INTRODUCTION

Atrial fibrillation (AF) is the most common type of sustained cardiac arrhythmia, with so-called rotors as possible driving sources.[1-3] These rotors form dynamical organizing centers supporting self-sustained electrical waves spiralling around excitable, yet inexcited cores.[4] AF can be terminated by the introduction of permanent tissue lesions, *i.e.* lines of conduction block, through catheter ablation therapy, which is now widely used for the treatment of both paroxysmal and persistent AF.[5,6] These lesions either prevent AF by blocking electrical activation at specific sites to eliminate focal triggers, or terminate AF by interrupting the pathway of reentrant waves. The most common ablation strategy for preventing AF is anatomy-guided and concerns the electrical isolation of pulmonary veins, a known source of these focal triggers.[7] This therapy results in an overall success rate of ≥ 80% in paroxysmal AF patients. However, such anatomy-guided ablation is less successful in non-paroxysmal patients.[8] Ablation of AF in these patients is a complex issue. Over the years many strategies for ablation were proposed, which, in addition to pulmonary vein isolation, included targeting of complex fractionated atrial electrograms and ganglionated plexi.[9] Recently, a new ablation strategy for AF has emerged with the rotor itself as prime target. This strategy involves the identification of a rotor by computational mapping, followed by local ablation at its organizing center, or core region.[10, 11] A number of clinical studies has indicated that such rotor-guided ablation could indeed terminate ongoing AF. Although this strategy has drawn a lot of attention, many of its fundamental aspects remain yet unexplored, including its mode of termination. Thus far, the effects of such precise local blocking of electrical propagation on rotor termination have only been studied in detail in computer models.[12-15] Insights from biologically active cardiac tissue are still lacking because conventional research tools do not allow precise spatiotemporally controlled induction of block. We have been able to take this first step by using light-gated depolarizing ion channels and patterned illumination to create light-controlled conduction blocks in cardiac tissue of any size and shape and at any desired location. Through this method, called optogenetics, we could (i) induce a stable rotor at a pre-defined location in neonatal rat atrial cardiomyocyte (nraCMC) monolayers and (ii) investigate its termination by inducing local conduction blocks of different configurations including or excluding the rotor core.

MATERIALS AND METHODS

Cultures preparation

All animal experiments were reviewed and approved by the Animal Experiments Committee of the Leiden University Medical Center and conformed to the Guide for the Care and Use of Laboratory Animals as stated by the US National Institutes of Health.

Monolayer and low-density cultures of neonatal rat atrial cardiomyocytes (nraCMCs) were established as previously described.[16] Briefly, 5% isoflurane was used to anesthetize 2-days-old Wistar rats. After rapid excision of the heart, the atria were carefully separated from the ventricles, then cut into small pieces and dissociated in a solution containing 450 U/ml collagenase type I (Worthington, Lakewood, NJ) and 18,75 Kunitz/ml DNase I (Sigma-Aldrich,

St. Louis, MO). The resulting cell suspension was transferred to Primaria-coated culture dishes (Becton Dickinson, Breda, the Netherlands) and incubated for 120 minutes in a humidified incubator at 37°C and 5% CO_2 to allow selective adhesion of non-nraCMCs. The non-attached cells (mainly nraCMCs) were filtered through a cell strainer (70 µm pore size; Corning Life Sciences, Amsterdam, the Netherlands) and seeded on round glass coverslips (15 mm diameter; Thermo Fisher Scientific Gerhard Menzel, Braunschweig, Germany) coated with fibronectin (100 µg/ml; Sigma-Aldrich). The cells were seeded at densities of 0.3-8×10^5 cells/well of a 24-well culture plate (Corning Life Sciences) depending on the assay. To minimize proliferation of the remaining non-nraCMCs, the cultures were treated with Mitomycin-C (10 µg/ml; Sigma-Aldrich) for 2 hours.[17] The cultures were incubated in an atmosphere of humidified 95% air- 5% CO_2 at 37°C. Culture medium was daily refreshed, and consisted of a 1:1 mixture of low-glucose Dulbecco's modified Eagle's medium (Thermo Fisher Scientific, Bleiswijk, the Netherlands) and Ham's F10 medium (MP Biomedicals, Santa Ana, CA) supplemented with 5% heat-inactivated horse serum (Thermo Fisher Scientific), 1× penicillin-streptomycin (Thermo Fisher Scientific), 2% bovine serum albumin (BSA) (Sigma-Aldrich) and sodium ascorbate (Sigma-Aldrich) to a final concentration of 0.4 mM.

Lentiviral (LV) vector production and transduction

LV particles encoding the L132C mutant of *Chlamydomonas reinhardtii* channelrhodopsin-2 (also known as Ca^{2+}-translocating channelrhodopsin [CatCh]), were produced in 293T cells from LV shuttle plasmid pLV.GgTnnt2.CatCh~eYFP.WHVPRE, as detailed elsewhere.[18] pLV.GgTnnt2.CatCh~eYFP.WHVPRE is a derivative of LV shuttle plasmid pLV.MHCK7. CatCh~eYFP.WHVPRE containing the chicken Tnnt2 promoter instead of the MHCK7 promoter in order to restrict transgene expression to cardiomyocytes. The LV particles were purified and concentrated by ultracentrifugation, suspended in phosphate-buffered saline (PBS) containing 1% BSA and stored at -80°C until use. At day 4 of culture, nraCMC monolayers were incubated for 20-24 h with LV particles at a dose resulting in homogeneous transduction of nearly 100% of the cells. Next, the cultures were washed once with PBS, given fresh culture medium and kept under culture conditions for 3-4 additional days. The transduction efficiency in the monolayer cultures was determined by visualization of the enhanced yellow fluorescent protein (eYFP) using a Nikon Eclipse 80i fluorescence microscope (Nikon Instruments Europe, Amstelveen, the Netherlands) after fixation of the cells with PBS/4% methanol-free formaldehyde (Thermo Fisher Scientific).

Immunocytology

Low-density nraCMC cultures (0.3×10^5 cells/15-mm glass coverslip) were fixed in PBS/4% methanol-free formaldehyde (Thermo Fisher Scientific), permeabilized with PBS/0.1% Triton X-100 and stained with a primary antibody directed against sarcomeric α-actinin (mouse IgG1, clone EA-53; Sigma-Aldrich). Incubation with the primary antibody (1:200 dilution in PBS+0.1% donkey serum) was performed overnight at 4°C, while the corresponding Alexa

Fluor 568-conjugated secondary antibody (Life Technologies; 1:400 dilution) was allowed to bind for 3 hours at room temperature (RT). Nuclear counterstaining was performed at RT for 10 minutes with 10 μg/ml Hoechst 33342 (Life Technologies) in PBS. After each processing step, cells were washed thrice with PBS. Coverslips were mounted in Vectashield mounting medium (Vector Laboratories, Burlingame, CA). Images were acquired with the Nikon Eclipse 80i fluorescence microscope. Immunostaining was performed on 3 independent cultures.

Optical mapping and optogenetic targeting

Optical voltage mapping was used to investigate the effects of local optogenetic targeting of rotors (*i.e.* induction of local conduction block) in CatCh-expressing nraCMC monolayers on day 7 of culture. Electrical activation was visualized using the voltage-sensitive dye di-4-ANBDQBS (52.5 μM final concentration; ITK diagnostics, Uithoorn, the Netherlands), which was excited by side illumination using a 150 W halogen light source (HL-151; SciMedia, Costa Mesa, CA) linked to a Semrock excitation filter (FF01-650/54-27, Semrock, Rochester, NY), while the emitted light was selected with an emission filter (pass >715 nm, FF01-715/LP-25, Semrock). Optical data were captured using a MiCAM ULTIMA-L imaging system (SciMedia) and analyzed with BrainVision Analyzer 1101 software (Brainvision, Tokyo, Japan). CatCh was locally activated by a patterned illumination device (Polygon400; Mightex Systems, Toronto, ON) that was connected to a 470-nm, high-power collimator light-emitting diode (LED) source (50 W, type-H, also from Mightex Systems), driven by a STG2004 stimulus generator (Multichannel Systems, Reutlingen, Germany). Accompanying PolyLite software (Mightex) was used to control the location and shape of the area of illumination, CatCh activation and conduction block. Light irradiance was measured using a PM100D optical power meter (Thorlabs, Munich, Germany). Before local optogenetic targeting, a single stable rotor was induced at the center of the monolayer by a light-based S1-S2 cross-field stimulation and monolayers were randomly assigned to either focal circular or linear configuration. Cycle length (CL) was determined as the time between 2 subsequent beats during sustained reentry. Action potential duration at 80% repolarization (APD_{80}) and conduction velocity (CV) during sustained reentry were spatial averages of three measurements per culture. Moreover, to minimize noise artifacts, a spatial averaging filter with 3×3 convolution kernel was used. Diastolic interval (DI) was defined as CL-APD_{80}, wavelength (λ) was expressed as CV×APD_{80}. Cultures showing stable rotors for >6 s were exposed to different patterns of illumination for 250 and 500 ms at 0.3 mW/mm^2 to create local conduction blocks at the site of interest. Since during the light-on period a shift in the baseline signal was observed, a drift filter was applied to allow optical voltage trace data interpretation while the derivative filter was used to visualize electrical propagation.

Patch-clamp recordings

For patch experiments, isolated nraCMCs were bathed in modified Tyrode's solution containing 126 mM NaCl, 5.4 mM KCl, 1.8 mM $CaCl_2$, 1 mM $MgCl_2$,11 mM glucose, 10 mM HEPES (pH adjusted to 7.4 with NaOH). Patch electrodes were pulled from borosilicate glass capillaries

and fire polished. Pipettes were fabricated with a P30 micropipet puller (Sutter Instruments, Novato, CA) and had a resistance of 2.4-3.0 MΩ when filled with the following solution: 80 mM L-aspartic acid potassium salt, 40 mM KCl, 8 mM NaCl 5.5 mM glucose, 5 mM HEPES, 1 mM MgCl2, 4 mM Mg-ATP, 0.1 mM Na_3-GTP (pH adjusted to 7.2 with KOH). CatCh-expressing nraCMCs were identified via epifluorescence using an Axiovert 35 inverted phase-contrast and fluorescence microscope (Carl Zeiss, Sliedrecht, the Netherlands). For current clamp experiments, only eYFP-positive, contracting nraCMCs were measured. Optical stimulation of these cells was performed with light from an incorporated LED module (blue [470 nm] collimated LED for Zeiss Axioskop, 1000 mA, Thorlabs). Recordings were performed at room temperature (20-22°C) using the whole-cell voltage clamp configuration with an Axopatch 700B amplifier controlled by pCLAMP 10.3 (Axon Instruments, Union City, CA). Currents were acquired with a low-pass filter of 10 kHz and digitized at 20 kHz using a Digidata 1440A A-D converter (Axon instruments). Voltages were corrected for liquid junction potentials. Steady-state depolarized membrane potentials were determined at the end of the light pulses.

Statistical analysis

Optical voltage data were expressed as mean ± SD. Comparison between 2 groups was performed with Student's t-test. Differences were considered statistically significant at $p<0.05$. Statistical analyses were performed with GraphPad Prism 7.01 (GraphPad Software, La Jolla, CA) software.

Acquisition and analysis of patch clamp data were performed using Clampfit 10.3 (Axon instruments), Excel 2010 (Microsoft, Seattle, WA) and GraphPad Prism 7.01 software. Data are presented as mean ± SEM.

RESULTS

CatCh expression and activation in nraCMCs

Immunocytological analysis of low-density nraCMC cultures transduced with LV.GgTnnt2. CatCh-eYFP~WHVPRE (see vector map shown in Supplementary Figure 1A) showed that CatCh expression occurred only in nraCMCs, *i.e.* α-actinin$^+$ cells (Figure 1A). To investigate the electrophysiological consequences of CatCh activation, whole-cell voltage- and current-clamp experiments were performed on single nraCMCs. Voltage-clamp recordings demonstrated that upon illumination with 470-nm light, at an intensity of 6 mW/mm^2 for 500 or 250 ms, a robust CatCh inward photocurrent was generated at resting membrane potentials of ~ -70 mV (n=7) (Figure 1B). More importantly, current-clamp experiments revealed the ability to induce prolonged depolarization by establishing a stable voltage plateau of -39 ± 4.9 and -41 ± 4.5 mV upon illumination for 250 and 500 ms, respectively (n=6; Figure 1C). The duration of the depolarized state was determined by the duration of the light pulses (Figure 1C). Taken together, these findings indicate that, given the significant upward shift in membrane potential upon illumination, electrical activation of nraCMCs could be blocked (*i.e.* the cells could be rendered temporary unexcitable) by prolonged activation of CatCh. Next, CatCh-expressing nraCMCs were used to create confluent monolayers (see Supplementary Figure 1B) to induce and target rotors.

Induction of a single stable rotor in nraCMC monolayers

With the aim to investigate the anti-arrhythmic effects of localized blocking of electrical activation near the rotor core region, a single and stable rotor was induced in nraCMC monolayers by a light-based S1-S2 cross-field stimulation (see Movie 1). Monolayers were optogenetically paced via patterned illumination of a 3-mm square area near the culture boundary using a brief light pulse (10 ms; 470 nm). The emerging S1 wave spread from the site of stimulation with a convex repolarization front.

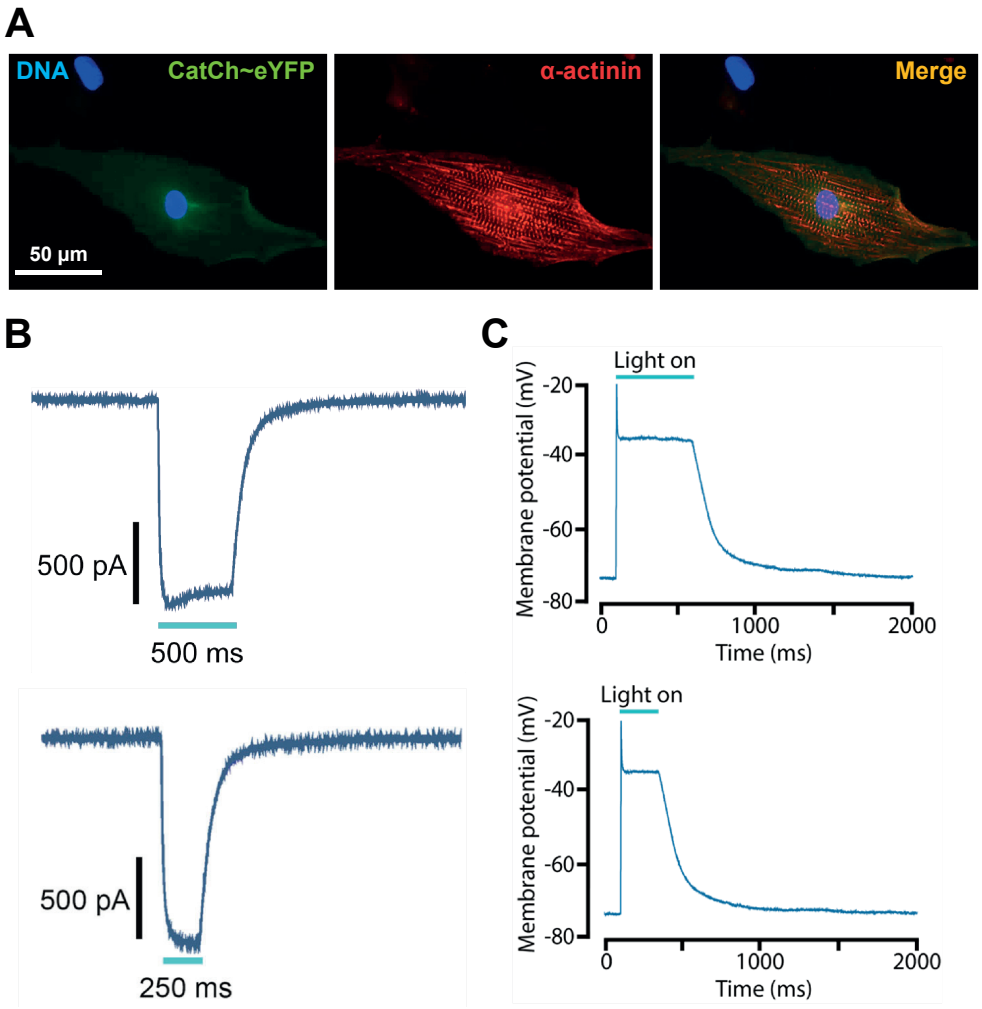

Figure 1. CatCh expression and activation in nraCMCs. A, Immunocytological staining of low-density CatCh-expressing nraCMC cultures for α-actinin^{+} (red), showing CatCh localization at the sarcolemma (green). B, Typical inward photocurrent evoked at a resting membrane potential of -70 mV by exposure of single CatCh-expressing nraCMCs to a 500- (top) or 250-ms (bottom) 470-nm light pulse (n=7). C, Representative membrane potential recordings of CatCh-expressing nraCMCs upon 470-nm light stimulation for 500- (top) or 250-ms (bottom), (n=6).

Circa 50 ± 10 ms later, a second light stimulus, S2 (20 ms; 470 nm), was applied to one half of the monolayer, perpendicular to the S1 repolarization front, such that, approximately one quarter of the culture remained excitable. This allowed the S2 stimulus to initiate a wave with a break at the interface between the excitable (non-illuminated, non-refractory) region and the temporary unexcitable (illuminated and therefore refractory) part of the monolayer (Figure 2A-B). With this protocol, a single rotor was induced in 100% of the monolayers (23 out of 23). Importantly, all these rotors were i) stable in time and space (see Figure 2B and C), and ii) centrally positioned in the monolayer (see Figure 2A and C). Thus, a robust *in vitro* model was created for studying the effects of local conduction blocks on atrial rotors in a unique and systematic manner.

Effects of core region targeting with circular conduction blocks

First, the effects of a circular conduction block at the site of the rotor core region were investigated. To this end, this region was targeted (*i.e.* focally illuminated; 470 nm, 0.3 mW/mm^2, 500 ms) with circular configurations of increasing diameter (3-, 6- or 12-mm, see Movies 2-4).

Upon local illumination, and therefore local activation of CatCh, two important simultaneously occurring phenomena could be observed: (i) emergence of a new electrical wave and (ii) formation of a functional conduction block (Figure 3A). During propagation, this new wave encountered both the activation and repolarization fronts of the existing rotor.

While its collision with the activation front of the existing rotor led to annihilation, interaction between the emergent wave and the repolarization front of this rotor led to the development of a new reentrant wave. This wave anchored to the illuminated area where a functional conduction

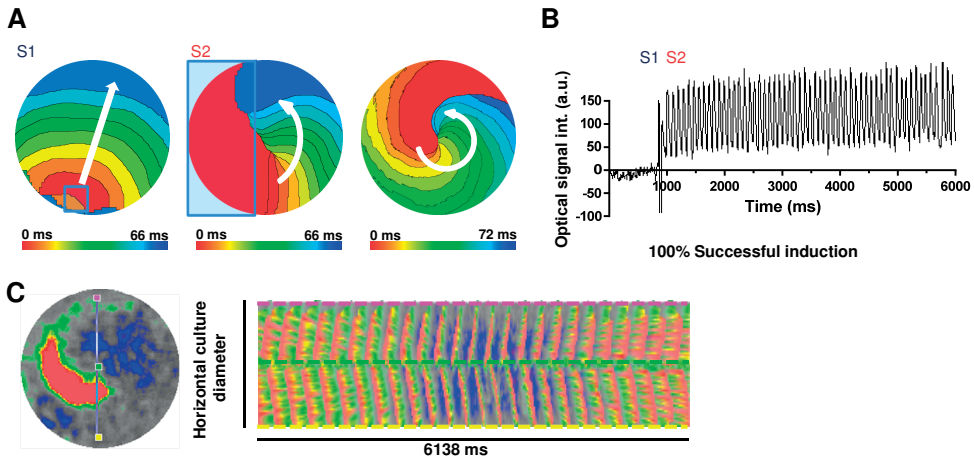

Figure 2. Optogenetic induction of a single, centralized and stable rotor. A and B, Representative activation maps (A) and optical trace (B) of a CatCh-expressing monolayer subjected to S1-S2 cross-field light stimulation to induce a single stable rotor at the center of the monolayer. C, Typical line scan analysis across a CatCh-expressing monolayer indicating that the rotor is stable in both space and time.

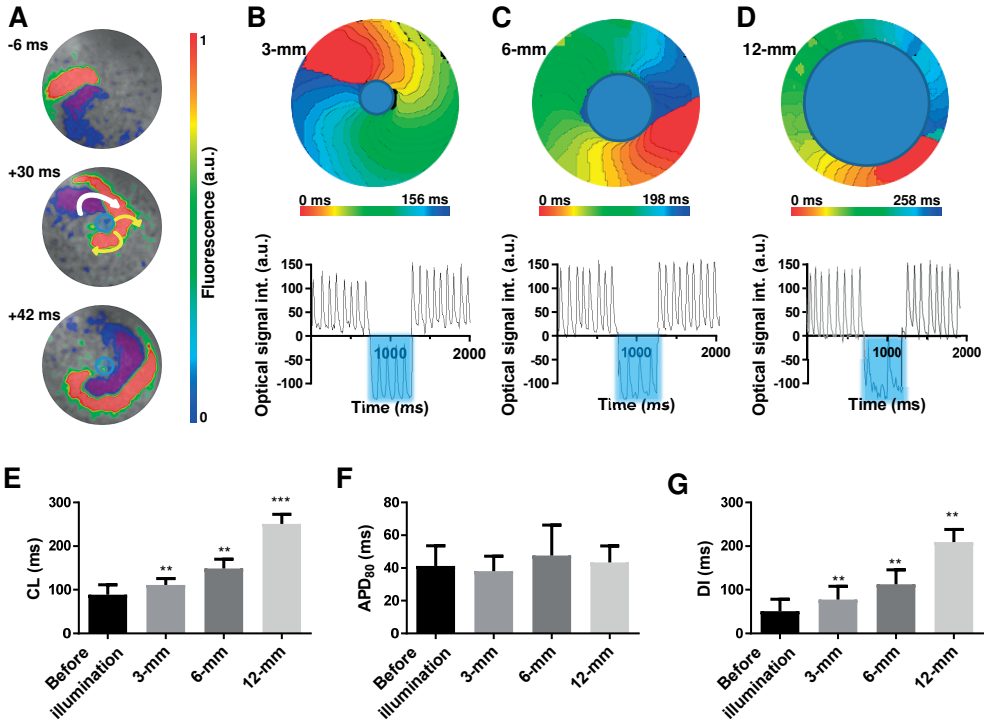

Figure 3. Effects of core region targeting with circular conduction blocks. A, Snapshots of optical signal before (upper panel) and during exposure (middle and bottom panel) to 470-nm light, showing the two typical phenomena occurring upon illumination: appearance of a new wave (indicated by yellow arrows) that interact with the existing reentrant wave (white arrows) and creation of a functional conduction block at the site of optical stimulation. B, C and D, Representative activation maps during 500-ms exposure to 470-nm light with centrally located circular shapes (blue shading) of 3- (B, top), 6- (C, top) or 12-mm in diameter (D, top). During illumination, the emerging wave anchors to the light-induced functional conduction block, thereby converting functional into anatomical reentrant activity. The corresponding optical signal traces recorded before, during and after light exposure are shown below the activation maps. E, F and G, Effect of circular conduction blocks (of 3-, 6- and 12-mm in diameter) at the rotor core region on (E) cycle length (CL), (F) action potential duration at 80% repolarization (APD_{80}), and (G) diastolic interval (DI). **P<0.01; ***P<0.001.

block was induced (Figure 3B, C, and D), thereby maintaining arrhythmic activity. Thus, instead of terminating the rotor, optogenetic targeting of the rotor core region converted functional into so-called anatomical reentry. Electrophysiological characterization of the electrical activity before and during illumination revealed a significant and diameter-dependent increase in CL (CL_{bi}=82±20; $CL_{3\text{-}mm}$=111.5±14.5; $CL_{6\text{-}mm}$=149.5±21; $CL_{12\text{-}mm}$=251±22; P(CL_{bi} vs $CL_{3\text{-}6\text{-}12\text{-}mm}$) <0.01; Figure 3E). APD_{80} did not show any significant difference (Figure 3F). Finally, there was a significant and diameter-dependent prolongation of the DI (DI_{bi}=49±24; $DI_{3\text{-}mm}$=77±30; $DI_{6\text{-}mm}$=113±33; $DI_{12\text{-}mm=}$209±28; P(DI_{bi} vs $DI_{3\text{-}6\text{-}12\text{-}mm}$)<0.01; Figure 3G) (n=8).

Effects of core region targeting with linear conduction blocks

Next, the effects of a linear conduction block at the rotor core region were investigated. To this purpose, a focal and central line (1 × 8 mm) was illuminated crossing the core region but not reaching one of the unexcitable boundaries of the culture (Figure 4A). Again the emergent new waves interacted with the existing rotor and replaced it by a new electrical wave that anchored to the light-induced functional conduction block, thereby maintaining arrhythmic activity (Figure 4B-C and Movie 5). However, when the length of this illuminated line was increased to 16 mm to connect the core region with both unexcitable boundaries of the culture (Figure 5A), all rotors were terminated (15 out of 15; Figure 5B and Movie 6).

Mechanistically, the local block of electrical activation forced both the existing reentrant wave and the light-induced emergent wave to drift along the line of block and towards the unexcitable boundaries of the culture, where they collided and vanished (Figure 5C). On the contrary, no termination occurred when monolayer-spanning lines of block did not include the core region (Figure 6B and Movie 7).

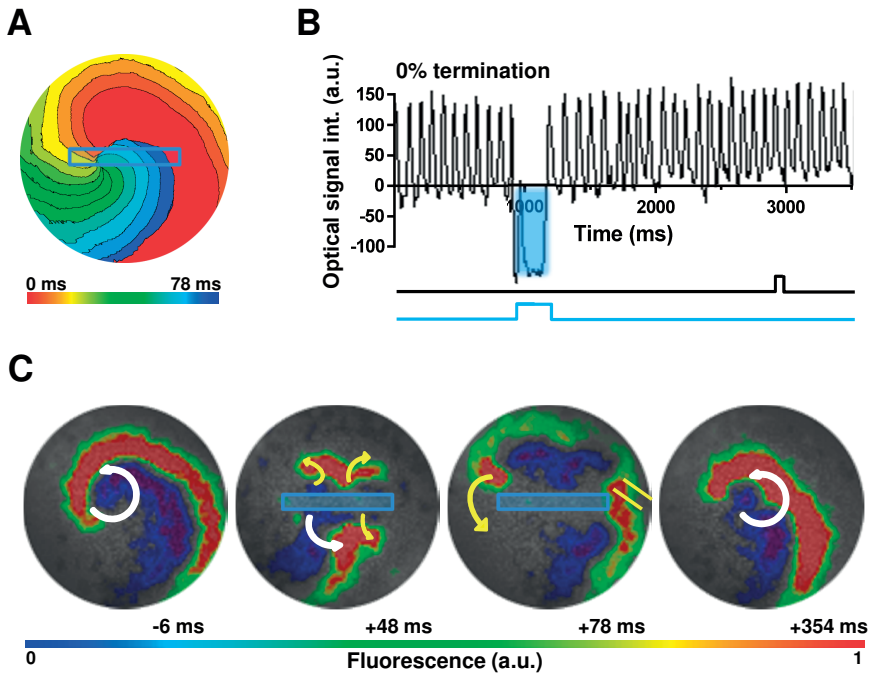

Figure 4. Effects of core region targeting with a linear conduction block not reaching any unexcitable boundaries. A, Activation map showing a single stable rotor and the area (blue shading) that will be exposed to light to induce a functional conduction block. B, Representative optical trace recorded before, during and after induction of conduction block by 250-ms exposure to 470-nm light. C, Snapshots of optical signal before and during light exposure showing unsuccessful rotor termination. The new waves (yellow arrows), emerge from the illuminated region and interact with the existing reentrant wave (white arrows), resulting in anchoring of a new wave to the light-induced conduction block, thereby maintaining arrhythmic activity.

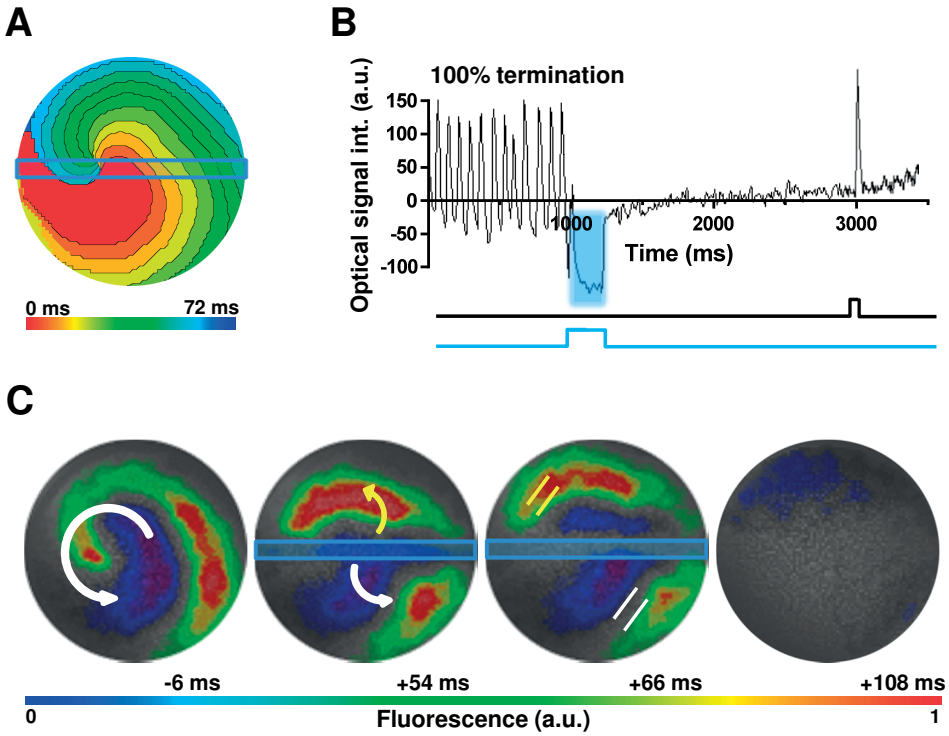

Figure 5. Effects of core region targeting with a linear conduction block reaching two opposite unexcitable boundaries. A, Activation map showing the position of the rotor core region and the area (blue shading) where light will be applied. B, Representative optical trace obtained before, during and after 250-ms exposure to 470-nm light. C, Snapshots of optical signal before and during light exposure showing successful rotor termination. Localized blocking of electric activity forces both the existing reentrant wave (in white arrows) and the light-induced emergent wave (yellow arrows) to drift toward the unexcitable boundaries in the culture, with which they collide.

In such cases, the emergent wave interfered with the existing rotor, leading to destabilization of its core. The rotor itself, however, survived and was attracted towards the site of optical stimulation (Figure 6C). Based on the success of the monolayer-spanning and rotor core-crossing linear configurations, we repeated the experiment with an illuminated line of 1 × 8 mm targeting the rotor core region and only one culture boundary (Figure 7A). Also with this configuration, rotor termination could be observed in 100% of the cases (Figure 7B and Movie8).

Both the original reentrant wave and the new wave followed the line of block and thereby collided with the unexcitable boundary of the culture and disappeared (Figure 7C).

In all cases, one electrical stimulus was applied 1.75 s after illumination (indicated by a black line) to confirm, in case of termination, the ability of the monolayers to be reactivated (Figure 5B and 7B).

Taken together these findings show that local targeting of a rotor without reaching to an unexcitable boundary, *i.e.* the creation of a circular or linear conduction block at the rotor

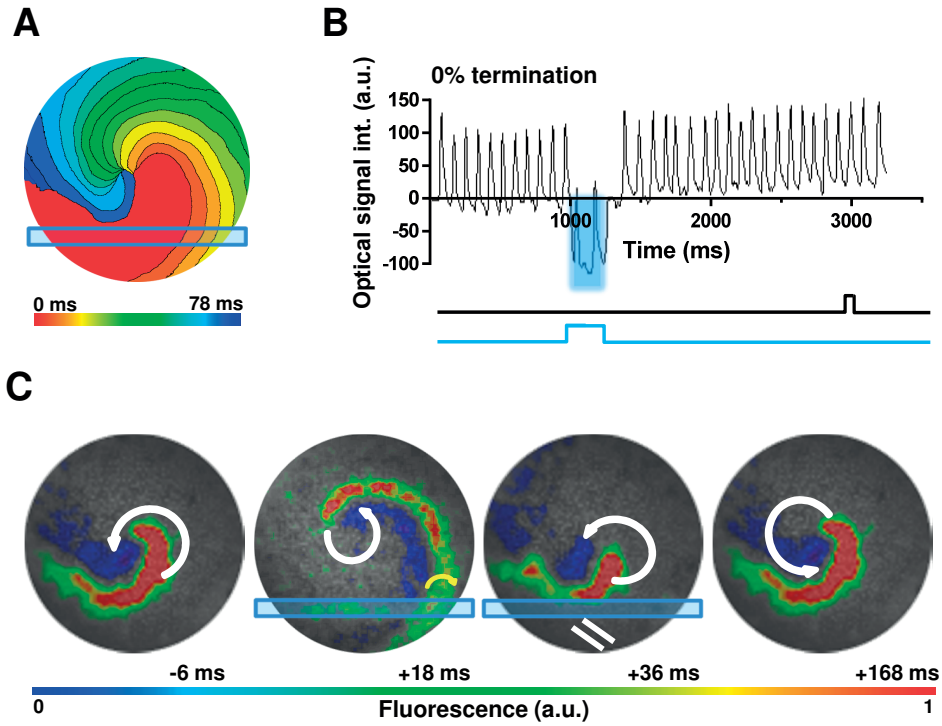

Figure 6. Effects of localized targeting away from the rotor core region with a linear conduction block reaching two opposite unexcitable boundaries. A, Activation map showing the location of the rotor core region with respect to the area (blue shading) that will be exposed to light. B, Representative optical traces registered before, during and after 250-ms exposure to 470-nm light. C, Snapshots of optical signal before and during light exposure showing unsuccessful rotor termination. The emergent wave (yellow arrows) interferes with the existing reentrant activity (in white arrows), leading to core destabilization and attraction towards the site of illumination, without causing arrhythmia termination.

core region in atrial CMC monolayers, does not lead to rotor termination. Instead, as long as the conduction block is present, the arrhythmic activity is maintained by so-called anatomical reentry albeit at a lower activation frequency. Here it is shown that for rotor termination by localized targeting, a line of conduction block should be created that is spanning from the rotor core region to at least one unexcitable boundary.

DISCUSSION

In this study, we investigated rotor termination in monolayers of nraCMCs by optogenetically blocking electrical activation at or near the rotor core region. Our findings reveal that an essential requirement for termination is the creation of a line of conduction block that is spanning from the rotor core region to at least one unexcitable boundary. Such localized targeting of the rotor forces the reentrant wave to propagate along the line of block to eventually collide into the unexcitable boundary, after which normal activation can regain.

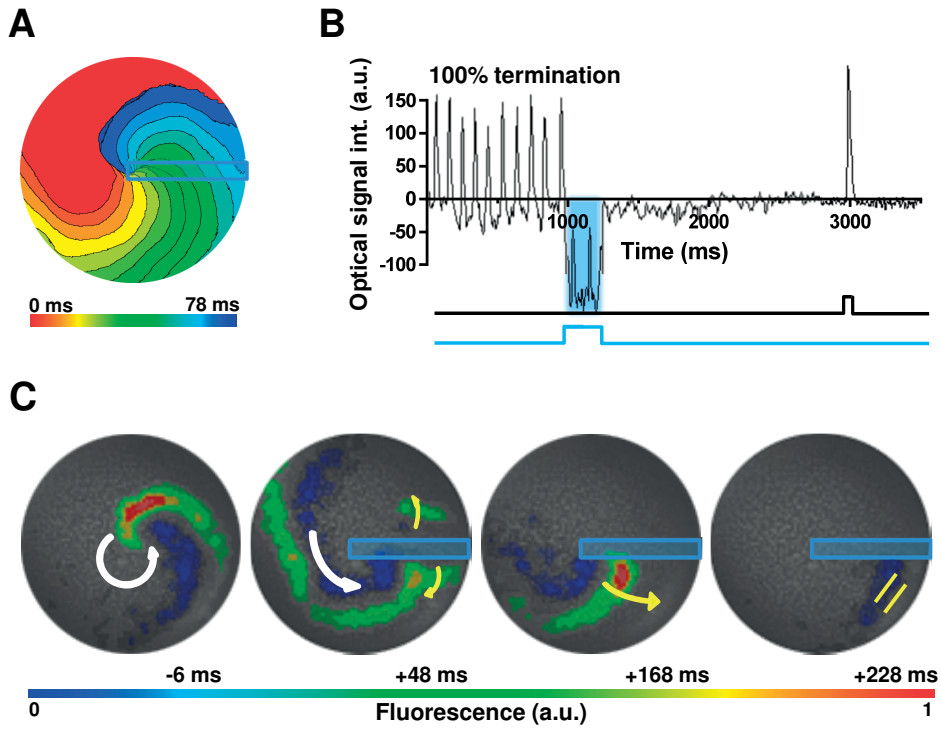

Figure 7. Effects of core region targeting with a linear conduction block reaching only one unexcitable boundary. A, Activation map showing the location of the core region of a single reentrant circuit and the location of the linear shape (blue shading) exposed to light. B, Optical traces recorded before, during and after 250-ms exposure to 470-nm light. C, Snapshots of optical signal before and during light exposure showing rotor termination. Both the original rotor (indicated by white arrows) and the new wave (in yellow arrows) follow the contour of the line where the conduction block is created, anchor and collide with the unexcitable boundary of the culture.

Optogenetic control of cardiac electrical function

In the past few years, optogenetics has emerged as a unique technology to modulate cardiac electrical function.[16, 19-25] This technology relies on forced expression of light-sensitive proteins whose activity can be precisely controlled in time and space by illumination. Optogenetic modulation of heart function was first proven in zebrafish by the stimulation and inhibition of electrical activation via brief and prolonged illumination, respectively.[19] Afterward, similar effects were also shown in rodent cardiomyocytes, both in monolayers and in intact hearts.[22] Here, brief light exposure caused membrane depolarization at the site of illumination, creating a supra-threshold stimulus for excitation, leading to action potential initiation and subsequent propagation out of the illuminated area. In the present study, we made use of the unique features of optical stimulation and inhibition of electrical activation to induce a single stable rotor. This was achieved by combining patterned illumination with a light-based pacing strategy, adapted from the well-established *in silico* S1-S2 cross-field stimulation protocol. This not only allowed

us to predetermine the location of the rotor core region, but also enabled us to target the rotor core region at a spatiotemporal resolution that could not be reached prior to the introduction of optogenetics. The possibility to induce a single stable rotor *in vitro* via S1-S2 cross-field stimulation has been previously described by Lim *et al*, who instead relied on the use of custom-made electrodes.[26] Our approach has, however, several technical advantages compared to the electrode-based method since it (i) allows better monitoring via optical mapping, owing to the absence of visually obstructive electrodes, and (ii) is more flexible in inducing rotors of predetermined chirality, at the desired location within the culture.

Recently, in addition to optical pacing, the ability to optogenetically terminate ventricular tachyarrhythmias in whole rat and mouse hearts expressing light-gated ion channels has been demonstrated.[23-25] Of those studies, Crocini *et al* used transgenic mice expressing *Chlamydomonas reinhardtii* channelrhodopsin-2 mutant H143R in the heart to investigate optogenetic induction of local conduction block for termination of ventricular tachycardia. Induction of 3 opposing lines of local block by patterned illumination resulted in arrhythmia termination with less energy than was required for arrhythmia termination by global illumination. In contrast to their more complex whole heart model, our 2D model and experimental setup allowed precise and predetermined optogenetic targeting of the actual arrhythmia driver, like induction of conduction block only in the core region of a rotor. Their study nevertheless confirms that local conduction blocks created by local activation of light-gated depolarizing ion channels allow termination of ongoing arrhythmias in the rodent heart.[25] Furthermore, optogenetic manipulation of anatomical reentry in ventricular tissue slices has been investigated in a previous study from our research group.[27] In this study, CatCh expression and its local activation, through patterned illumination, induced a local and reversible conduction block in the reentrant pathway, which allowed termination of reentrant activity.[16] In another study, members of our research team have shown optogenetic termination of multiple reentrant circuits in monolayers of nraCMC cardiomyocytes by global activation of CatCh, which caused spiral wave drift and collisions. In the present study, we activated CatCh only locally in monolayers of nraCMC in order to investigate rotor termination by precise, spatially restricted optogenetic blocking of electrical activation at or near the rotor core region.

Optogenetic targeting of the rotor core region

One of our main motivations to study localized targeting of atrial rotors via the afore-mentioned approach was to improve our mechanistic understanding of so-called rotor-guided ablation. This ablation strategy involves the identification of the rotor core region by computational mapping, followed by targeted ablation of this particular site. Several recent clinical studies have indicated that such rotor-guided ablation could indeed favor termination of ongoing AF.[10, 11, 13] However, the way by which the rotors are terminated remains poorly understood. This is partly due to a lack of dedicated research models and tools, especially regarding the precision by which a conduction block can be created in a certain shape at a particular location. In the present study, patterned illumination was used to activate CatCh with the aim to first induce a single

stable rotor, and then block electrical activation regionally in order to mimic the conduction block resulting from an ablation procedure. We used optogenetic induction of conduction block to tackle this issue of precision, and by doing so showed that localized targeting of the core region without reaching an unexcitable boundary does not terminate the arrhythmia. Computer simulations both support and contradict these findings. Likely due to the homogeneity of our monolayers, factors responsible for rotor drift and meandering were mostly absent resulting in highly stable rotors. These results are in line with *in silico* studies. In those studies, Spector *et al* and Carrick *et al* pointed out that the concept of using ablation to transect a spatially fixed reentrant pathway is understandable, but that creation of focal lesions targeting the rotor core region seems less obvious.[12, 14] In contrast, a recent *in silico* study conducted by Rappel *et al* showed that focal ablation near the core region could indeed terminate a rotor if the cardiac tissue was affected by structural and functional heterogeneities.[13] It may, therefore, be relevant to include such heterogeneities, like gradients in excitability and non-homogenous distribution of cardiac fibroblasts, in future optogenetic *in vitro* experiments to investigate their role in rotor termination by focal ablation. However, these heterogeneities will most likely also affect the stability of the rotor, both in time and space, which will no longer allow a precisely controlled and systematic study into localized targeting of rotors. In this context, our finding that linear blocks extending from the core region to at least one unexcitable boundary of homogeneous monolayers resulted in termination of all rotors is of particular interest. With the aim to optimize AF ablation efficacy, while limiting the tissue damage resulting from ablation, these results may help to further refine rotor-based ablation strategies.

In our study, the optogenetic induction of a conduction block to mimic the electrophysiological consequences of an ablation lesion, also resulted in the emergence of a new wave of excitation that played a crucial role in rotor termination by interfering with the existing reentrant wave and introducing new electrical activity into the monolayers. The clinical relevance of these ablation-induced waves remains yet to be clarified. Nevertheless, it is well known that ablation comes with cell death and could involve local thermic responses, which may cause transient and local membrane depolarization, causing ectopic activity.[28] Another interesting phenomenon that we observed in our experiments was the tendency of the light-induced functional conduction block to destabilize and attract nearby rotors. In these cases, the linear conduction block was established away from the core region of the rotor, which gradually drifted towards the area of conduction block although rotor termination did not occur. These findings are in line with the results of *in silico* studies by Defauw *et al*, who showed, by using the Ten Tusscher-Noble-Noble-Panfilov model for human ventricular tissue, that such interactions between the rotor core and the region of conduction block has important consequences for the dynamical behavior of the rotors and may result in their stabilization through conversion into anatomical reentry.[29] Regarding our results, more investigation is needed to determine whether and how localized targeting further away from the rotor core region may still lead to termination of arrhythmic activity.

Study limitations

The novel model presented in this study is a 2D model of atrial tachycardia based on a single stable rotor. This *in vitro* model obviously does not reproduce the structural and functional complexity of the intact heart and accompanying atrial arrhythmias, and therefore the results should be interpreted as such. Our model nonetheless did allow us to investigate the electrophysiological consequences of localized rotor targeting through optogenetic induction of conduction blocks, which now can be a stepping stone to future experiments on rotor targeting in more complex and realistic models of atrial tissue. Moreover, the temporary nature of the functional conduction block employed in this study does not allow investigating its role in preventing the formation of new rotors.

Conclusions

This study shows that localized targeting of rotors in atrial monolayers, by means of optogenetic induction of a conduction block at the site of the rotor core region, only leads to termination if the line of block reaches from the core region to at least one unexcitable boundary. Localized targeting with no involvement of such boundary merely forces the electrical waves to anchor to the conduction block, thereby sustaining arrhythmic activity based on anatomical reentry. These findings may therefore lead to a better understanding of the mechanisms involved in rotor destabilization and termination after localized ablation, and thus help to further improve AF ablation strategies.

ACKNOWLEDGMENTS

We thank Cindy Bart, Annemarie Kip and Serge A.I.P. Trines (Department of Cardiology, LUMC) for assistance with the animal experiments, LV production and constructive discussion, respectively.

FUNDING SOURCES

This work was supported by the Netherlands Organisation for Scientific Research (NWO, Vidi grant 91714336) and the European Research Council (ERC, Starting grant 716509, both to D.A.P.). Additional support was provided by Ammodo (to D.A.P. and A.A.F.d.V.).

DISCLOSURES

None.

REFERENCES

1. Chugh SS, Havmoeller R, Narayanan K, Singh D, Rienstra M, Benjamin EJ, Gillum RF, Kim YH, McAnulty JH, Jr., Zheng ZJ, Forouzanfar MH, Naghavi M, Mensah GA, Ezzati M, Murray CJ. Worldwide epidemiology of atrial fibrillation: a Global Burden of Disease 2010 Study. Circulation. 2014; 129:837-47.
2. Go AS, Hylek EM, Phillips KA, Chang Y, Henault LE, Selby JV, Singer DE. Prevalence of diagnosed atrial fibrillation in adults: national implications for rhythm management and stroke prevention: the AnTicoagulation and Risk Factors in Atrial Fibrillation (ATRIA) Study. JAMA. 2001; 285:2370-5.
3. Lloyd-Jones DM, Wang TJ, Leip EP, Larson MG, Levy D, Vasan RS, D'Agostino RB, Massaro JM, Beiser A, Wolf PA, Benjamin EJ. Lifetime risk for development of atrial fibrillation: the Framingham Heart Study. Circulation. 2004; 110:1042-6.
4. Pandit SV, Jalife J. Rotors and the dynamics of cardiac fibrillation. Circ Res. 2013; 112:849-62.
5. Mont L, Bisbal F, Hernandez-Madrid A, Perez-Castellano N, Vinolas X, Arenal A, Arribas F, Fernandez-Lozano I, Bodegas A, Cobos A, Matia R, Perez-Villacastin J, Guerra JM, Avila P, Lopez-Gil M, Castro V, Arana JI, Brugada J. Catheter ablation vs. antiarrhythmic drug treatment of persistent atrial fibrillation: a multicentre, randomized, controlled trial (SARA study). Eur Heart J. 2014; 35:501-7.
6. Pappone C, Augello G, Sala S, Gugliotta F, Vicedomini G, Gulletta S, Paglino G, Mazzone P, Sora N, Greiss I, Santagostino A, LiVolsi L, Pappone N, Radinovic A, Manguso F, Santinelli V. A randomized trial of circumferential pulmonary vein ablation versus antiarrhythmic drug therapy in paroxysmal atrial fibrillation: the APAF Study. J Am Coll Cardiol. 2006; 48:2340-7.
7. Pappone C, Oreto G, Rosanio S, Vicedomini G, Tocchi M, Gugliotta F, Salvati A, Dicandia C, Calabro MP, Mazzone P, Ficarra E, Di GC, Gulletta S, Nardi S, Santinelli V, Benussi S, Alfieri O. Atrial electroanatomic remodeling after circumferential radiofrequency pulmonary vein ablation: efficacy of an anatomic approach in a large cohort of patients with atrial fibrillation. Circulation. 2001; 104:2539-44.
8. Oral H, Pappone C, Chugh A, Good E, Bogun F, Pelosi F, Jr., Bates ER, Lehmann MH, Vicedomini G, Augello G, Agricola E, Sala S, Santinelli V, Morady F. Circumferential pulmonary-vein ablation for chronic atrial fibrillation. N Engl J Med. 2006; 354:934-41.
9. Kirchhof P, Calkins H. Catheter ablation in patients with persistent atrial fibrillation. Eur Heart J. 2017; 38:20-6.
10. Narayan SM, Krummen DE. Targeting Stable Rotors to Treat Atrial Fibrillation. Arrhythm Electrophysiol Rev. 2012; 1:34-8.
11. Narayan SM, Krummen DE, Shivkumar K, Clopton P, Rappel WJ, Miller JM. Treatment of atrial fibrillation by the ablation of localized sources: CONFIRM (Conventional Ablation for Atrial Fibrillation With or Without Focal Impulse and Rotor Modulation) trial. J Am Coll Cardiol. 2012; 60:628-36.
12. Carrick RT, Benson BE, Bates JH, Spector PS. Prospective, Tissue-Specific Optimization of Ablation for Multiwavelet Reentry: Predicting the Required Amount, Location, and Configuration of Lesions. Circ Arrhythm Electrophysiol. 2016;9.
13. Rappel WJ, Zaman JA, Narayan SM. Mechanisms for the Termination of Atrial Fibrillation by Localized Ablation: Computational and Clinical Studies. Circ Arrhythm Electrophysiol. 2015; 8:1325-33.
14. Spector PS, Correa de Sa DD, Tischler ES, Thompson NC, Habel N, Stinnett-Donnelly J, Benson BE, Bielau P, Bates JH. Ablation of multi-wavelet re-entry: general principles and in silico analyses. Europace. 2012; Suppl 5:v106-v111.
15. Ugarte JP, Tobon C, Orozco-Duque A, Becerra MA, Bustamante J. Effect of the electrograms density in detecting and ablating the tip of

the rotor during chronic atrial fibrillation: an in silico study. Europace. 2015; 17 Suppl 2:ii97-104.

16. Bingen BO, Engels MC, Schalij MJ, Jangsangthong W, Neshati Z, Feola I, Ypey DL, Askar SF, Panfilov AV, Pijnappels DA, de Vries AA. Light-induced termination of spiral wave arrhythmias by optogenetic engineering of atrial cardiomyocytes. Cardiovasc Res. 2014; 104:194-205.

17. Askar SF, Ramkisoensing AA, Schalij MJ, Bingen BO, Swildens J, van der Laarse A, Atsma DE, de Vries AA, Ypey DL, Pijnappels DA. Antiproliferative treatment of myofibroblasts prevents arrhythmias in vitro by limiting myofibroblast-induced depolarization. Cardiovasc Res. 2011; 90:295-304.

18. Feola I, Teplenin A, de Vries AA, Pijnappels DA. Optogenetic Engineering of Atrial Cardiomyocytes. Methods Mol Biol. 2016; 1408:319-31.

19. Arrenberg AB, Stainier DY, Baier H, Huisken J. Optogenetic control of cardiac function. Science. 2010; 330:971-4.

20. Nussinovitch U, Gepstein L. Optogenetics for in vivo cardiac pacing and resynchronization therapies. Nat Biotechnol. 2015; 33:750-4.

21. Nussinovitch U, Shinnawi R, Gepstein L. Modulation of cardiac tissue electrophysiological properties with light-sensitive proteins. Cardiovasc Res. 2014; 102:176-87.

22. Bruegmann T, Malan D, Hesse M, Beiert T, Fuegemann CJ, Fleischmann BK, Sasse P. Optogenetic control of heart muscle in vitro and in vivo. Nat Methods. 2010; 7:897-900.

23. Nyns EC, Kip A, Bart CI, Plomp JJ, Zeppenfeld K, Schalij MJ, de Vries AA, Pijnappels DA. Optogenetic termination of ventricular arrhythmias in the whole heart: towards biological cardiac rhythm management. Eur Heart J. 2017; 38:2132–2136.

24. Bruegmann T, Boyle PM, Vogt CC, Karathanos TV, Arevalo HJ, Fleischmann BK, Trayanova NA, Sasse P. Optogenetic defibrillation terminates ventricular arrhythmia in mouse hearts and human simulations. J Clin Invest. 2016; 126:3894-904.

25. Crocini C, Ferrantini C, Coppini R, Scardigli M, Yan P, Loew LM, Smith G, Cerbai E, Poggesi C, Pavone FS, Sacconi L. Optogenetics design of mechanistically-based stimulation patterns for cardiac defibrillation. Sci Rep. 2016; 6:35628.

26. Lim ZY, Maskara B, Aguel F, Emokpae R, Jr., Tung L. Spiral wave attachment to millimeter-sized obstacles. Circulation. 2006; 114:2113-21.

27. Watanabe M, Feola I, Majumder R, Jangsangthong W, Teplenin AS, Ypey DL, Schalij MJ, Zeppenfeld K, de Vries AA, Pijnappels DA. Optogenetic manipulation of anatomical re-entry by light-guided generation of a reversible local conduction block. Cardiovasc Res. 2017; 113:354-66.

28. Nath S, Lynch C, III, Whayne JG, Haines DE. Cellular electrophysiological effects of hyperthermia on isolated guinea pig papillary muscle. Implications for catheter ablation. Circulation. 1993; 88:1826-31.

29. Defauw A, Vandersickel N, Dawyndt P, Panfilov AV. Small size ionic heterogeneities in the human heart can attract rotors. Am J Physiol Heart Circ Physiol. 2014; 307:H1456-H1468.

SUPPLEMENTAL MATERIAL

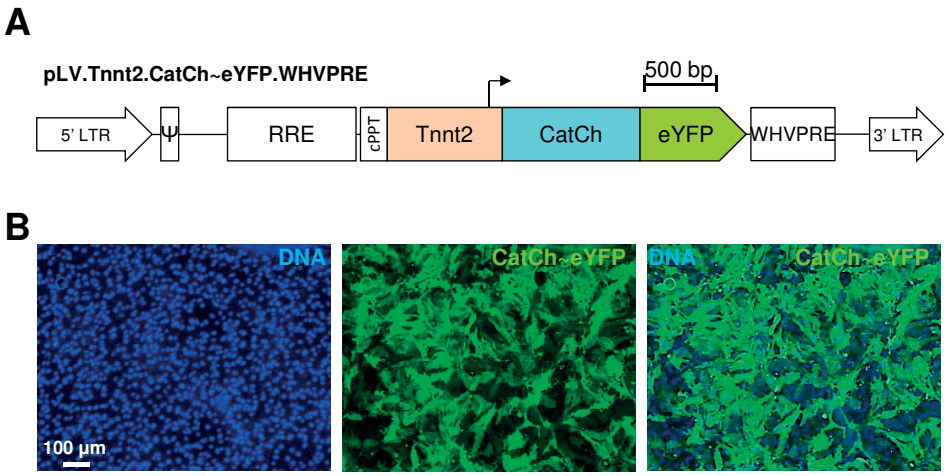

Supplementary figure 1. A, Structure of LV shuttle plasmid pLV.GgTnnt2.CatCh~eYFP.WHVPRE. B, Fluoromicrograph image of confluent Catch-expressing nraCMC monolayers showing homogenous transgene expression.

Movie 1. Induction of a single centralized stable rotor.

Movie 2. Effects of core region targeting with 3-mm circular conduction block.

Movie 3. Effects of core region targeting with 6-mm circular conduction block.

Movie 4. Effects of core region targeting with 12-mm circular conduction block.

Movie 5. Effects of core region targeting with a linear conduction block not reaching any unexcitable boundaries.

Movie 6. Effects of core region targeting with a linear conduction block reaching two opposite unexcitable boundaries.

Movie 7. Effects of localized targeting away from the rotor core region with a linear conduction block reaching two opposite unexcitable boundaries.

Movie 8. Effects of core region targeting with a linear conduction block reaching only one unexcitable boundary.